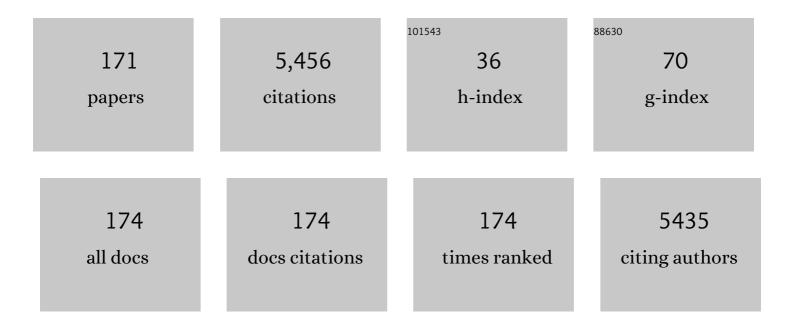
## Jennifer Wong-Leung

List of Publications by Year in descending order

Source: https://exaly.com/author-pdf/4813511/publications.pdf Version: 2024-02-01



#	Article	IF	CITATIONS
1	Electron-pinned defect-dipoles for high-performance colossal permittivity materials. Nature Materials, 2013, 12, 821-826.	27.5	784
2	Phase Perfection in Zinc Blende and Wurtzite Illâ^'V Nanowires Using Basic Growth Parameters. Nano Letters, 2010, 10, 908-915.	9.1	443
3	Mechanical deformation in silicon by micro-indentation. Journal of Materials Research, 2001, 16, 1500-1507.	2.6	234
4	Transmission electron microscopy observation of deformation microstructure under spherical indentation in silicon. Applied Physics Letters, 2000, 77, 3749-3751.	3.3	210
5	Selective-Area Epitaxy of Pure Wurtzite InP Nanowires: High Quantum Efficiency and Room-Temperature Lasing. Nano Letters, 2014, 14, 5206-5211.	9.1	198
6	Ultralow Surface Recombination Velocity in InP Nanowires Probed by Terahertz Spectroscopy. Nano Letters, 2012, 12, 5325-5330.	9.1	158
7	Gettering of copper to hydrogenâ€induced cavities in silicon. Applied Physics Letters, 1995, 66, 1231-1233.	3.3	123
8	High Efficiency Perovskite‣ilicon Tandem Solar Cells: Effect of Surface Coating versus Bulk Incorporation of 2D Perovskite. Advanced Energy Materials, 2020, 10, 1903553.	19.5	110
9	Indentation-induced damage in GaN epilayers. Applied Physics Letters, 2002, 80, 383-385.	3.3	107
10	Enhanced Minority Carrier Lifetimes in GaAs/AlGaAs Core–Shell Nanowires through Shell Growth Optimization. Nano Letters, 2013, 13, 5135-5140.	9.1	97
11	Ultra-micro-indentation of silicon and compound semiconductors with spherical indenters. Journal of Materials Research, 1999, 14, 2338-2343.	2.6	94
12	Mechanical deformation of InP and GaAs by spherical indentation. Applied Physics Letters, 2001, 78, 3235-3237.	3.3	94
13	Gettering of Au to dislocations and cavities in silicon. Applied Physics Letters, 1995, 67, 416-418.	3.3	85
14	Long minority carrier lifetime in Au-catalyzed GaAs/AlxGa1â^'xAs core-shell nanowires. Applied Physics Letters, 2012, 101, .	3.3	80
15	Polarity-Driven 3-Fold Symmetry of GaAs/AlGaAs Core Multishell Nanowires. Nano Letters, 2013, 13, 3742-3748.	9.1	80
16	Twinning Superlattice Formation in GaAs Nanowires. ACS Nano, 2013, 7, 8105-8114.	14.6	77
17	Capture cross sections of the acceptor level of iron–boron pairs in p-type silicon by injection-level dependent lifetime measurements. Journal of Applied Physics, 2001, 89, 7932-7939.	2.5	75
18	Nanoindentation-induced deformation of Ge. Applied Physics Letters, 2002, 80, 2651-2653.	3.3	70

#	Article	IF	CITATIONS
19	Tunable Polarity in a III–V Nanowire by Droplet Wetting and Surface Energy Engineering. Advanced Materials, 2015, 27, 6096-6103.	21.0	69
20	Gettering of nickel to cavities in silicon introduced by hydrogen implantation. Applied Physics Letters, 1995, 66, 1889-1891.	3.3	66
21	Influence of Interface Morphology on Hysteresis in Vaporâ€Deposited Perovskite Solar Cells. Advanced Electronic Materials, 2017, 3, 1600470.	5.1	63
22	Simultaneous Selective-Area and Vapor–Liquid–Solid Growth of InP Nanowire Arrays. Nano Letters, 2016, 16, 4361-4367.	9.1	57
23	Flow modulation epitaxy of hexagonal boron nitride. 2D Materials, 2018, 5, 045018.	4.4	57
24	Controlling the morphology, composition and crystal structure in gold-seeded GaAs <sub>1â^'x</sub> Sb <sub>x</sub> nanowires. Nanoscale, 2015, 7, 4995-5003.	5.6	56
25	Understanding the True Shape of Au-Catalyzed GaAs Nanowires. Nano Letters, 2014, 14, 5865-5872.	9.1	52
26	Nanowires Grown on InP (100): Growth Directions, Facets, Crystal Structures, and Relative Yield Control. ACS Nano, 2014, 8, 6945-6954.	14.6	51
27	Engineering the Photoresponse of InAs Nanowires. ACS Applied Materials & Interfaces, 2017, 9, 43993-44000.	8.0	49
28	Effects of rapid thermal annealing on device characteristics of InGaAsâ^•GaAs quantum dot infrared photodetectors. Journal of Applied Physics, 2006, 99, 114517.	2.5	45
29	Dynamic annealing in ion implanted SiC: Flux versus temperature dependence. Journal of Applied Physics, 2003, 94, 7112-7115.	2.5	44
30	Growth of Straight InAs-on-GaAs Nanowire Heterostructures. Nano Letters, 2011, 11, 3899-3905.	9.1	44
31	Solubility limit and precipitate formation in Al-doped 4H-SiC epitaxial material. Applied Physics Letters, 2001, 79, 2016-2018.	3.3	43
32	Engineering Ill–V Semiconductor Nanowires for Device Applications. Advanced Materials, 2020, 32, e1904359.	21.0	43
33	The precipitation of Fe at the Si–SiO2 interface. Journal of Applied Physics, 1998, 83, 580-584.	2.5	42
34	Effect of crystal orientation on the implant profile of 60 keV Al into 4H-SiC crystals. Journal of Applied Physics, 2003, 93, 8914-8917.	2.5	42
35	Ion mass effect on vacancy-related deep levels in Si induced by ion implantation. Physical Review B, 2002, 65, .	3.2	40
36	Tailoring GaAs, InAs, and InGaAs Nanowires for Optoelectronic Device Applications. IEEE Journal of Selected Topics in Quantum Electronics, 2011, 17, 766-778.	2.9	40

#	Article	IF	CITATIONS
37	Perovskite Photovoltaic Integrated CdS/TiO <sub>2</sub> Photoanode for Unbiased Photoelectrochemical Hydrogen Generation. ACS Applied Materials & Interfaces, 2018, 10, 23766-23773.	8.0	38
38	Ultrathin Ta <sub>2</sub> O <sub>5</sub> electron-selective contacts for high efficiency InP solar cells. Nanoscale, 2019, 11, 7497-7505.	5.6	38
39	Influence of rapid thermal annealing on a 30 stack InAs/GaAs quantum dot infrared photodetector. Journal of Applied Physics, 2003, 94, 5283.	2.5	37
40	InxGa1â^'xAs nanowires with uniform composition, pure wurtzite crystal phase and taper-free morphology. Nanotechnology, 2015, 26, 205604.	2.6	36
41	Suppression of interdiffusion in GaAs/AlGaAs quantum-well structure capped with dielectric films by deposition of gallium oxide. Journal of Applied Physics, 2002, 92, 3579-3583.	2.5	35
42	Proximity gettering of Au to ion beam induced defects in silicon. Nuclear Instruments & Methods in Physics Research B, 1995, 96, 253-256.	1.4	33
43	Low loss, thin p-clad 980-nm InGaAs semiconductor laser diodes with an asymmetric structure design. IEEE Journal of Quantum Electronics, 2003, 39, 625-633.	1.9	33
44	Separation of vacancy and interstitial depth profiles in ion-implanted silicon: Experimental observation. Applied Physics Letters, 2001, 78, 3442-3444.	3.3	32
45	Multiwavelength Single Nanowire InGaAs/InP Quantum Well Light-Emitting Diodes. Nano Letters, 2019, 19, 3821-3829.	9.1	32
46	Diffusion and transient trapping of metals in silicon. Physical Review B, 1999, 59, 7990-7998.	3.2	31
47	Ion-implantation-induced extended defect formation in (0001) and(112Â <sup>-</sup> 0)4Hâ^'SiC. Physical Review B, 2005, 71, .	3.2	31
48	Direct Observation of Charge-Carrier Heating at WZ–ZB InP Nanowire Heterojunctions. Nano Letters, 2013, 13, 4280-4287.	9.1	31
49	Interaction of defects and metals with nanocavities in silicon. Nuclear Instruments & Methods in Physics Research B, 2001, 178, 33-43.	1.4	29
50	Direct observation of voids in the vacancy excess region of ion bombarded silicon. Applied Physics Letters, 2001, 78, 2867-2869.	3.3	28
51	Spherical indentation of compound semiconductors. Philosophical Magazine A: Physics of Condensed Matter, Structure, Defects and Mechanical Properties, 2002, 82, 1931-1939.	0.6	28
52	A transmission electron microscopy study of defects formed through the capping layer of self-assembled InAsâ^•GaAs quantum dot samples. Journal of Applied Physics, 2006, 99, 113503.	2.5	28
53	Polarization Tunable, Multicolor Emission from Core–Shell Photonic III–V Semiconductor Nanowires. Nano Letters, 2012, 12, 6428-6431.	9.1	27
54	Unraveling the influence of CsCl/MACl on the formation of nanotwins, stacking faults and cubic supercell structure in FA-based perovskite solar cells. Nano Energy, 2021, 87, 106226.	16.0	27

#	Article	IF	CITATIONS
55	Fluence, flux, and implantation temperature dependence of ion-implantation-induced defect production in 4H–SiC. Journal of Applied Physics, 2005, 97, 033513.	2.5	26
56	Radial Growth Evolution of InGaAs/InP Multi-Quantum-Well Nanowires Grown by Selective-Area Metal Organic Vapor-Phase Epitaxy. ACS Nano, 2018, 12, 10374-10382.	14.6	26
57	The role of oxygen on the stability of gettering of metals to cavities in silicon. Applied Physics Letters, 1999, 75, 2424-2426.	3.3	25
58	Highly uniform InGaAs/InP quantum well nanowire array-based light emitting diodes. Nano Energy, 2020, 71, 104576.	16.0	23
59	Diffusion and trapping of Au to cavities induced by H-implantation in Si. Nuclear Instruments & Methods in Physics Research B, 1995, 106, 424-428.	1.4	22
60	Vacancy and interstitial depth profiles in ion-implanted silicon. Journal of Applied Physics, 2003, 93, 871-877.	2.5	22
61	Direct Observation of the Impurity Gettering Layers in Polysilicon-Based Passivating Contacts for Silicon Solar Cells. ACS Applied Energy Materials, 2018, 1, 2275-2282.	5.1	22
62	Gettering of platinum and silver to cavities formed by hydrogen implantation in silicon. Nuclear Instruments & Methods in Physics Research B, 1997, 127-128, 297-300.	1.4	21
63	Electrical characterization of the threshold fluence for extended defect formation in p-type silicon implanted with MeV Si ions. Applied Physics Letters, 1998, 72, 3044-3046.	3.3	21
64	High vertical yield InP nanowire growth on Si(111) using a thin buffer layer. Nanotechnology, 2013, 24, 465602.	2.6	21
65	InGaAsP as a Promising Narrow Band Gap Semiconductor for Photoelectrochemical Water Splitting. ACS Applied Materials & Interfaces, 2019, 11, 25236-25242.	8.0	21
66	Effect of ion mass on the evolution of extended defects during annealing of MeV ion-implanted p-type Si. Applied Physics Letters, 1999, 74, 1141-1143.	3.3	19
67	Defect formation and thermal stability of H in high dose H implanted ZnO. Journal of Applied Physics, 2013, 114, 083111.	2.5	19
68	CdS/TiO <sub>2</sub> photoanodes via solution ion transfer method for highly efficient solar hydrogen generation. Nano Futures, 2018, 2, 015004.	2.2	19
69	Solubility limits of dopants in 4H–SiC. Applied Surface Science, 2003, 203-204, 427-432.	6.1	18
70	Insights into Twinning Formation in Cubic and Tetragonal Multi-cation Mixed-Halide Perovskite. , 2020, 2, 415-424.		17
71	Effect of implant temperature on secondary defects created by MeV Sn implantation in silicon. Journal of Applied Physics, 2001, 89, 2556-2559.	2.5	16
72	Suppression of ion-implantation induced porosity in germanium by a silicon dioxide capping layer. Applied Physics Letters, 2016, 109, .	3.3	16

#	Article	IF	CITATIONS
73	The influence of cavities and point defects on boron diffusion in silicon. Applied Physics Letters, 1998, 72, 2418-2420.	3.3	15
74	lon implantation in 4H–SiC. Nuclear Instruments & Methods in Physics Research B, 2008, 266, 1367-1372.	1.4	15
75	Electric field assisted annealing and formation of prominent deep-level defect in ion-implanted n-type 4H-SiC. Applied Physics Letters, 2008, 92, .	3.3	15
76	Acceptor-like deep level defects in ion-implanted ZnO. Applied Physics Letters, 2012, 100, 212106.	3.3	15
77	Electronic comparison of InAs wurtzite and zincblende phases using nanowire transistors. Physica Status Solidi - Rapid Research Letters, 2013, 7, 911-914.	2.4	15
78	Efficient gettering of low concentrations of copper contamination to hydrogen induced nanocavities in silicon. Applied Physics Letters, 1998, 73, 2639-2641.	3.3	14
79	Identification of hydrogen related defects in proton implanted float-zone silicon. EPJ Applied Physics, 2003, 23, 5-9.	0.7	14
80	Understanding the Chemical and Structural Properties of Multiple-Cation Mixed Halide Perovskite. Journal of Physical Chemistry C, 2019, 123, 26718-26726.	3.1	14
81	Microstructural difference between platinum and silver trapped in hydrogen induced cavities in silicon. Applied Physics Letters, 1998, 72, 2713-2715.	3.3	13
82	Photoluminescence response of ion-implanted silicon. Applied Physics Letters, 2006, 89, 181917.	3.3	13
83	The role of arsine in the self-assembled growth of InAsâ•GaAs quantum dots by metal organic chemical vapor deposition. Journal of Applied Physics, 2006, 99, 044908.	2.5	13
84	Effect of boron on interstitial-related luminescence centers in silicon. Applied Physics Letters, 2010, 96, 051906.	3.3	13
85	Selectivity of nanocavities and dislocations for gettering of Cu and Fe in silicon. Applied Physics Letters, 2001, 78, 2682-2684.	3.3	12
86	Formation of precipitates in heavily boron doped 4H-SiC. Applied Surface Science, 2006, 252, 5316-5320.	6.1	12
87	Ion Implantation Processing and Related Effects in SiC. Materials Science Forum, 2006, 527-529, 781-786.	0.3	11
88	Ion implantation induced defects in ZnO. Physica B: Condensed Matter, 2012, 407, 1481-1484.	2.7	11
89	Understanding the role of facets and twin defects in the optical performance of GaAs nanowires for laser applications. Nanoscale Horizons, 2021, 6, 559-567.	8.0	11
90	Transmission electron microscopy characterization of secondary defects created by MeV Si, Ge, and Sn implantation in silicon. Journal of Applied Physics, 2000, 88, 1312-1318.	2.5	10

#	Article	IF	CITATIONS
91	The formation, migration, agglomeration and annealing of vacancy-type defects in self-implanted Si. Journal of Materials Science: Materials in Electronics, 2007, 18, 695-700.	2.2	9
92	The effect of nitridation on the polarity and optical properties of GaN self-assembled nanorods. Nanoscale, 2018, 10, 11205-11210.	5.6	9
93	Effects of high temperature annealing on defects and luminescence properties in H implanted ZnO. Journal Physics D: Applied Physics, 2014, 47, 342001.	2.8	8
94	Analysis of semiconductors by ion channelling: Applications and pitfalls. Nuclear Instruments & Methods in Physics Research B, 1998, 136-138, 453-459.	1.4	7
95	Study of defects in ion-implanted silicon using photoluminescence and positron annihilation. Physica B: Condensed Matter, 2003, 340-342, 738-742.	2.7	7
96	Growth and Characterization of Self-Assembled InAs/InP Quantum Dot Structures. Journal of Nanoscience and Nanotechnology, 2010, 10, 1525-1536.	0.9	7
97	Selective Intermixing of InGaAs/GaAs Quantum Dot Infrared Photodetectors. IEEE Journal of Quantum Electronics, 2011, 47, 577-590.	1.9	7
98	Improving the Morphology and Crystal Quality of AlN Grown on Two-Dimensional hBN. Crystal Growth and Design, 2020, 20, 1811-1819.	3.0	7
99	Exploring the band structure of Wurtzite InAs nanowires using photocurrent spectroscopy. Nano Research, 2020, 13, 1586-1591.	10.4	7
100	Spherical indentation of compound semiconductors. Philosophical Magazine A: Physics of Condensed Matter, Structure, Defects and Mechanical Properties, 2002, 82, 1931-1939.	0.6	7
101	The role of Fe on the crystallisation of α-Si3N4 from amorphous Si–N formed by ion implantation. Nuclear Instruments & Methods in Physics Research B, 1999, 148, 534-539.	1.4	6
102	The crystallisation of deep amorphous wells in silicon produced by ion implantation. Nuclear Instruments & Methods in Physics Research B, 2001, 175-177, 164-168.	1.4	6
103	Growth and Characterisation of InAs/GaAs Quantum Dots Grown by MOCVD. , 0, , .		6
104	InAs quantum dots grown on InGaAs buffer layers by metal–organic chemical vapor deposition. Journal of Crystal Growth, 2005, 281, 290-296.	1.5	6
105	Ion irradiation-induced disordering of semiconductors: defect structures and applications. Philosophical Magazine, 2005, 85, 677-687.	1.6	6
106	Identification by photoluminescence and positron annihilation of vacancy and interstitial intrinsic defects in ion-implanted silicon. Journal of Applied Physics, 2006, 100, 073501.	2.5	6
107	Self-assembled Au nanoparticles in SiO2 by ion implantation and wet oxidation. Journal of Applied Physics, 2009, 106, 103526.	2.5	6
108	Equilibrium shape of nano-cavities in H implanted ZnO. Applied Physics Letters, 2015, 106, .	3.3	6

#	Article	IF	CITATIONS
109	Photoluminescence Excitation Spectroscopy of Diffused Layers on Crystalline Silicon Wafers. IEEE Journal of Photovoltaics, 2016, 6, 746-753.	2.5	6
110	Highly regular rosette-shaped cathodoluminescence in GaN self-assembled nanodisks and nanorods. Nano Research, 2020, 13, 2500-2505.	10.4	6
111	Role of defects and grain boundaries in the thermal response of wafer-scale hBN films. Nanotechnology, 2021, 32, 075702.	2.6	6
112	Rutherford backscattering and channeling study of Au trapped at cavities in silicon. Nuclear Instruments & Methods in Physics Research B, 1996, 118, 34-38.	1.4	5
113	Defect formation due to the crystallization of deep amorphous volumes formed in silicon by mega electron volt (MeV) ion implantation. Journal of Materials Research, 2001, 16, 3229-3237.	2.6	5
114	Separation of vacancy and interstitial depth profiles in proton- and boron-implanted silicon. Nuclear Instruments & Methods in Physics Research B, 2002, 186, 334-338.	1.4	5
115	Tuning the bandgap of InAs quantum dots by selective-area MOCVD. Journal Physics D: Applied Physics, 2008, 41, 085104.	2.8	5
116	Comparison of the structural properties of Zn-face and O-face single crystal homoepitaxial ZnO epilayers grown by RF-magnetron sputtering. Journal of Applied Physics, 2017, 121, .	2.5	5
117	Tuning the crystal structure and optical properties of selective area grown InGaAs nanowires. Nano Research, 2022, 15, 3695-3703.	10.4	5
118	Defect Trapping and Precipitation Processes During Annealing of Cu and Au Implanted Si. Materials Research Society Symposia Proceedings, 1994, 354, 255.	0.1	4
119	Mechanical Deformation of Crystalline Silicon During Nanoindentation. Materials Research Society Symposia Proceedings, 2000, 649, 8101.	0.1	4
120	Cathodoluminescence visualisation of local thickness variations of GaAs/AlGaAs quantum-well tubes on nanowires. Nanotechnology, 2020, 31, 424001.	2.6	4
121	Defect Evolution in Hydrogen Implanted Silicon. , 1996, , 832-836.		4
122	Impact of Halide Anions in CsX (X = I, Br, Cl) on the Microstructure and Photovoltaic Performance of FAPbI <sub>3</sub> â€Based Perovskite Solar Cells. Solar Rrl, 2022, 6, .	5.8	4
123	Microstructure of Irradiated Silicon. Materials Research Society Symposia Proceedings, 1994, 373, 543.	0.1	3
124	Voids and Nanocavities in Silicon. Topics in Applied Physics, 2009, , 113-146.	0.8	3
125	Dopant effects on the photoluminescence of interstitial-related centers in ion implanted silicon. Journal of Applied Physics, 2012, 111, 094910.	2.5	3
126	Zn precipitation and Li depletion in Zn implanted ZnO. Applied Physics Letters, 2016, 109, 022102.	3.3	3

#	Article	IF	CITATIONS
127	The Influence of Cavities and Point Defects on Cu Gettering and B'Diffusion in Si. Materials Research Society Symposia Proceedings, 1997, 469, 457.	0.1	2
128	Non-Equilibrium Formation Of Silicon Nitride During Both Ball Milling And Ion Bombardment. Materials Research Society Symposia Proceedings, 1997, 481, 439.	0.1	2
129	Efficiency of dislocations and cavities for gettering of Cu and Fe in silicon. Nuclear Instruments & Methods in Physics Research B, 2001, 175-177, 154-158.	1.4	2
130	A comparison of extended defect formation induced by ion implantation in (0001) and (112̄0) 4H-SiC. Physica B: Condensed Matter, 2003, 340-342, 132-136.	2.7	2
131	Effect of boron on formation of interstitialâ€related luminescence centres in ion implanted silicon. Physica Status Solidi (A) Applications and Materials Science, 2011, 208, 620-623.	1.8	2
132	Anomalous Diffusion of Intrinsic Defects in K+ Implanted ZnO using Li as Tracer. Materials Research Society Symposia Proceedings, 2012, 1394, 75.	0.1	2
133	Direct correlation of R-line luminescence with rod-like defect evolution in ion-implanted and annealed silicon. MRS Communications, 2012, 2, 101-105.	1.8	2
134	Anderson-like localization in ultrathin nanocomposite alloy films on polymeric substrates. Scripta Materialia, 2012, 67, 866-869.	5.2	2
135	How InAs crystal phase affects the electrical performance of InAs nanowire FETs. , 2014, , .		2
136	Critical Temperature for the Conversion from Wurtzite to Zincblende of the Optical Emission of InAs Nanowires. Journal of Physical Chemistry C, 2017, 121, 16650-16656.	3.1	2
137	Impurity Gettering by Diffusion-doped Polysilicon Passivating Contacts for Silicon Solar Cells. , 2018, ,		2
138	Facet-Related Non-uniform Photoluminescence in Passivated GaAs Nanowires. Frontiers in Chemistry, 2020, 8, 607481.	3.6	2
139	Transient Diffusion and Gettering of Au and Cu to Cavities in Si. Materials Research Society Symposia Proceedings, 1995, 378, 273.	0.1	1
140	Gettering of metals to nanocavities in silicon. , 0, , .		1
141	Effect of Implant Temperature on Extended Defects Craeted by Ion Implantation in Silicon. Defect and Diffusion Forum, 2000, 183-185, 163-170.	0.4	1
142	Response to "Comment on â€~Separation of vacancy and interstitial depth profiles in ion-implanted silicon: Experimental observation' ―[Appl. Phys. Lett. 80, 1492 (2002)]. Applied Physics Letters, 2002, 80 1494-1495.	0, 3.3	1
143	Asymmetric design of semiconductor laser diodes: thin p-clad and low divergence InGaAs/AlGaAs/GaAs devices. , 0, , .		1
144	Ion implantation effects in silicon with high carbon content characterised by photoluminescence. Physica B: Condensed Matter, 2003, 340-342, 714-718.	2.7	1

#	Article	IF	CITATIONS
145	Point defect engineered Si sub-bandgap light-emitting diodes. Proceedings of SPIE, 2007, , .	0.8	1
146	Achieving a narrow size distribution of Au particles at a precise depth in SiO <sub>2</sub> by segregation of Au precipitates. Nanotechnology, 2009, 20, 185603.	2.6	1
147	Spectral tuning of InGaAs/GaAs quantum dot infrared photodetectors using selective-area intermixing. , 2010, , .		1
148	Comparison between implanted boron and phosphorus in silicon wafers , 2010, , .		1
149	Mn Implantation for New Applications of 4H-SiC. Materials Science Forum, 0, 717-720, 221-224.	0.3	1
150	InP nanowires grown by SA-MOVPE. , 2012, , .		1
151	Characterisation of the Subthreshold Damage in MeV Ion Implanted p Si. Materials Research Society Symposia Proceedings, 1998, 510, 411.	0.1	0
152	Interactions of Point Defects and Impurities With Open Volume Defects in Silicon. Materials Research Society Symposia Proceedings, 2000, 647, 1.	0.1	0
153	Strain relaxation in rapid thermally annealed InAs/GaAs quantum dot infrared photodetectors. , 0, , .		Ο
154	Spatial selectivity of impurity free vacancy disordering using different dielectric layers for photonic/optoelectronic integrated circuits. , 0, , .		0
155	Proton Irradiation Induced Intermixing in In_xGa_1-xAs/InP Quantum Wells. , 0, , .		0
156	Compound semiconductor optoelectronics research at the Australian National University. , 2005, , .		0
157	Controlled nucleation of InAs/GaAs and InGaAs/GaAs quantum dots for optoelectronic device integration. , 0, , .		0
158	Structural and optical properties of H implanted ZnO. , 2012, , .		0
159	Improvement of minority carrier lifetime in GaAs/Al <inf>x</inf> Ga <inf>1−x</inf> As core-shell nanowires. , 2012, , .		Ο
160	Growth and characterization of GaAs <inf>1−x</inf> Sb <inf>x</inf> nanowires. , 2012, , .		0
161	Influence of growth temperature and V/III ratio on Au-assisted In <inf>x</inf> Ga <inf>1−x</inf> As nanowires. , 2012, , .		0
162	Measuring the electrical properties of semiconductor nanowires using terahertz conductivity spectroscopy. Proceedings of SPIE, 2013, , .	0.8	0

#	Article	IF	CITATIONS
163	Probing the critical electronic properties of III–V nanowires using optical pump-terahertz probe spectroscopy. , 2013, , .		0
164	High performance GaAs/AlGaAs radial heterostructure nanowires grown by MOCVD. , 2013, , .		0
165	Compound semiconductor nanowires for optoelectronic devices. , 2013, , .		0
166	InP-based radial heterostructures grown on [100] nanowires. , 2014, , .		0
167	Sidewall evolution in VLS grown GaAs nanowires. , 2014, , .		0
168	Semiconductor nanowires in terahertz photonics: From spectroscopy to ultrafast nanowire-based devices. , 2017, , .		0
169	Large area hexagonal boron nitride coatings for SERS applications with silver nanoparticles. , 2019, , .		0
170	Engineering III-V nanowires for optoelectronics: from epitaxy to terahertz photonics. , 2018, , .		0
171	Engineering Ill–V Nanowires for Optoelectronics: From Visible to Terahertz. , 2019, , .		Ο